*17th World Conference on Earthquake Engineering, 17WCEE*
*Sendai, Japan - September 13th to 18th 2020*

# PROBABILISTIC DAMAGE INDEX FUNCTIONS FOR OLD WOODEN HOUSES BASED ON PERIOD-DEPENDENT SPECTRUM INTENSITY

T. Furukawa[(1)], Y. Mori[(2)], R. Usami[(3)], Y. Mizutani[(4)], and H. Idota[(5)]

[(1)] *Graduate Student, Nagoya University, Nagoya, Japan, furukawa.taishi@g.mbox.nagoya-u.ac.jp*
[(2)] *Professor, Nagoya University, Nagoya, Japan, yasu@nuac.nagoya-u.ac.jp*
[(3)] *Graduate Student, Nagoya University, Nagoya, Japan, g.usa0709@gmail.com*
[(4)] *Graduate Student, Nagoya University, Nagoya, Japan, mizutani.yukari@j.mbox.nagoya-u.ac.jp*
[(5)] *Professor, Nagoya Institute of Technology, Nagoya, Japan, idota@nitech.ac.jp*

## *Abstract*

There is widespread awareness in seismic-prone countries about the necessity to upgrade the seismic performance of old buildings and houses for disaster mitigation; however, upgrading occurs at a very slow space. In order to support the decision-making of the owners on upgrading, appropriate seismic risk information specific to their house should be conveyed so that the effect of seismic upgrading on risk reduction can be compared in a continuous manner.

Risk information of a house can be estimated using seismic hazard information and a fragility curve. However, these basic information generally is not quite specific to the house. For example, seismic hazard has been often estimated for a mesh with a side length of 250 m or so, but site characteristics and accordingly seismic hazard would not be uniform within the mesh. Fragility curves for houses classified according to the period of construction have been proposed based on field survey following the past earthquakes. Such fragility curves are useful to estimate damage of houses as a whole within a mesh for which seismic hazard is estimated. Yet, the seismic performance of houses should be different from each other even if they are constructed during the same period.

Recently, a technique to estimate seismic hazard for each house taking site characteristics is being developed. In order to effectively utilize such detailed estimation, some of the authors have developed probabilistic damage index of a wooden house in Japan as a function of PGV, taking specific information related to the damage level of the house such as characteristic of site conditions and seismic performance of the house based on the seismic diagnosis into account. However, the dispersion of the function is relatively large because the structural characteristics other than its strength of the houses are not considered.

The purpose of this research is to develop more reliable damage index function. Natural period-dependent spectrum intensity is considered as the ground motions intensity in order to take the structural characteristics of houses into account. Three existing two-story wooden houses with typical traditional seismic resistance element in the 1960th and the 1970th are considered. These houses are upgraded or downgraded by adding or removing walls and/or braces to model houses with various level of load-carrying capacity. Non-linear dynamic analyses are conducted using a number of ground motions simulated considering soil conditions and types of earthquakes, and the models of the median and the dispersion of damage index functions are developed on the basis of the statistics of the maximum inter-story drift ratio. The validity of the proposed functions is investigated using a number of recorded ground motions.

*Keywords: non-conforming wooden house; seismic risk information; decision making; upgrading; sense of values*

 



## 1. Introduction

There is widespread awareness in seismic-prone countries about the necessity to upgrade the seismic performance of old buildings and houses for disaster mitigation [1, 2]. Strategies for managing seismic risk have been studied extensively [3, 4, 5]; however, upgrading is occurring at a very slow space. To support decision-making by the owners on upgrading, appropriate seismic risk information specific to their houses should be conveyed, so that the effect of seismic upgrading on risk reduction can be assessed in a continuous manner.

Risk information on a house can be estimated using seismic hazard information and fragility curves. However, such basic information is normally not quite specific to the house. For example, seismic hazard has been often estimated for a mesh with a side length of approximately 250 m etc., but site characteristics and seismic hazard would not be uniform within the mesh. Fragility curves have been proposed for houses classified according to the period of construction, based on field survey conducted on the past earthquakes [6, 7]. Such fragility curves are useful in estimating the damage of houses as a whole within a mesh for which seismic hazard is estimated. Yet, the seismic performance of houses would vary even if they are constructed during the same period.

Recently, a technique to estimate seismic hazard for each house, considering the site characteristics, has been developed [8]. To effectively use such detailed information, some authors have developed the probabilistic damage index for a wooden house in Japan as a function of PGV, taking specific information related to the damage level of the house, such as characteristics of the site conditions and seismic performance of the house, based on seismic diagnosis [9]. However, the dispersion of the function is relatively large, because the structural characteristics other than the strength of the houses are not considered.

The purpose of this research is to develop a more reliable damage index function. Natural period-dependent spectrum intensity [10] is considered as the intensity of ground motions so as to take the structural characteristics of the houses into account. Nonlinear dynamic analyses (NDA) of two-degrees-of-freedom (2-DOF) systems are conducted by modeling wooden houses using a number of ground motions simulated considering the soil conditions and types of earthquakes. Then, the models of the median and dispersion damage index functions are developed based on the statistics of the maximum inter-story drift ratio. The validity of the proposed functions is investigated using a number of recorded ground motions.

## 2. Analytical Models and Ground Motions

In this study, the results of NDA conducted in reference [9] are also used. The analytical models and ground motions used in the NDA are described in this section.

### 2.1 Structural performance of wooden houses

The structural performance of a wooden house is measured by a seismic grade, $I_g$, given based on seismic diagnosis. $I_g$ is estimated as the ratio of the sum of the load-carrying capacities of earthquake-resisting elements, such as walls and braces, to the required load-carrying capacity prescribed in Japan's present-day seismic design code. The load-carrying capacity of an element is evaluated by its equivalent potential energy under a certain deformation. An $I_g$ value of 1.0 indicates that the house meets the present-day design requirements.

### 2.2 Structural model

The basic models considered here are based on three existing two-story wooden houses with tiled roofs and wooden braces (cross section: 90 mm × 30 mm), which were the typical seismic resistance elements used in construction during the 1960s and 1970s [11]. By adding or removing walls and/or braces, these houses are upgraded or downgraded to have $I_g$ values of 0.3, 0.4, 0.7, 1.0, 1.3, and 2.0. To achieve an $I_g$ value of 2.0, the roof tiles are replaced with lighter materials. These houses are modeled as 2-DOF systems with a damping factor of 0.05.



 



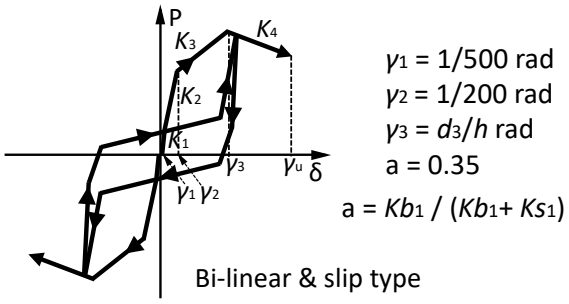


Fig. 1. Bi-linear & slip force displacement characteristics

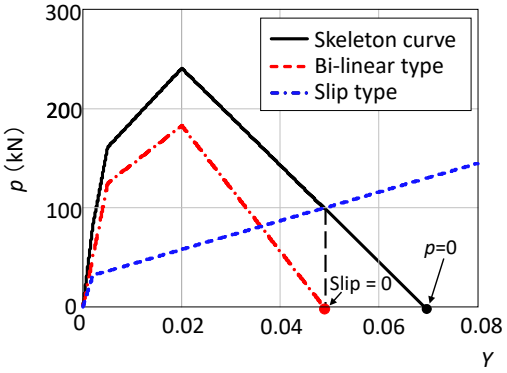


Fig. 2. Backbone curve

Table 1. Natural periods of 2-DOF systems [s]

| Model | $I_g$ | | | | | |
|---|---|---|---|---|---|---|
| | 0.3 | 0.4 | 0.7 | 1.0 | 1.3 | 2.0 |
| A | 0.74 | 0.70 | 0.47 | 0.35 | 0.28 | 0.25 |
| B | 0.71 | 0.61 | 0.43 | 0.31 | 0.25 | 0.23 |
| C | 0.67 | 0.58 | 0.40 | 0.30 | 0.24 | 0.22 |
| $T_L$ | 0.70 | 0.60 | 0.40 | 0.30 | 0.25 | 0.20 |

Table 2. Load-bearing capacity of existing wooden houses

| Seismic grade and index of load-bearing capacity | Takada et al., 2010 | Isoda et al., 2007 |
|---|---|---|
| $I_g$ | 0.56 | 1.25 |
| $P_e^*/P_d$ | 1.7 | 3.0 |
| $P_a/P_d$ | 1.19 | 2.10 |

The force-displacement characteristics of the systems are modeled as a combination of bi-linear and slip models, as shown in Fig. 1 [11]; this combined model is referred to hereafter as the BS model. The backbone curve is obtained as the sum of the values in the bi-linear and slip models up to the point at which the slip model loses its load-carrying capacity; the backbone curve slopes downward and maintains the same negative slope beyond this point, as shown in Fig. 2.

In this study, an advanced normalized characteristic loop (NCL) model [12] is adopted for the hysteresis loop instead of the BS model. The parameters of the NCL model are determined such that the shape of the loop is similar to that of the BS model and the area of the loop is equal to that of the BS model. The first natural periods of the 2-DOF systems are summarized in Table 1.

## 2.3 Adjustment of load-bearing capacity

Because of conservative estimation, the load-bearing capacity of the existing wooden houses estimated by a pull-down experiment, $P_e^*$, tends to be higher than that estimated by seismic diagnosis, $P_d$. Table 2 lists the ratio of the load-bearing capacity estimated by the pull-down experiment $P_e^*$ to that estimated by the seismic diagnosis $P_d$ [13, 14]. In rare cases, the ratio obtained experimentally could be large. Assuming that (a) the non-exceedance probability of the ratio obtained by these experiments is 0.9, (b) the ratio of $P_e$ to $P_d$ is normally distributed with a coefficient of variation equal to 0.33, and (c) $P_d = P_e$ when $I_g < 0.30$, the load-carrying capacity of the structural model, $P_a$, is determined as the mean of $P_e$ from the following equation.



 



$$\frac{P_a}{P_d} = \begin{cases} 1.0 & (I_g \leq 0.3) \\ 1.51 I_g + 0.13 + 0.13/I_g & (0.3 < I_g < 1.25) \\ 2.10 & (I_g \geq 1.25) \end{cases} \quad (1)$$

## 2.4 Ground motion characteristics

To investigate the effect of different ground motion characteristics and the related uncertainty, six sets of 50 ground motions for different types of earthquakes (interplate and intraplate) and soil conditions (hard, medium, and soft) are simulated [15].

In the spectral domain, the time history of a given ground motion can be characterized by its power spectral density and phase spectrum. The authors assume that the power spectral density is lognormally distributed, and the mean power spectral density, $S(\omega; \omega_g)$, is modeled using a modified Kanai-Tajimi model [16], expressed as

$$S(\omega; \omega_g) = \frac{1 + 4h_g^2 \left(\frac{\omega}{\omega_g}\right)^2}{\left[1 - \left(\frac{\omega}{\omega_g}\right)^2\right]^2 + 4h_g^2 \left(\frac{\omega}{\omega_g}\right)^2} \cdot \frac{\left(\frac{\omega}{\omega_f}\right)^2}{\left[1 - \left(\frac{\omega}{\omega_f}\right)^2\right]^2 + 4h_f^2 \left(\frac{\omega}{\omega_f}\right)^2} S_0(\omega_g) \quad (2)$$

where $\omega$ is the circular frequency; $\omega_g$ is the dominant circular frequency of the soil; and $h_g$, $\omega_f$, and $h_f$ are the parameters that determine the spectral shape. Further, $S_0(\omega_g)$ is the spectral intensity given by

$$S_0(\omega_g) = \frac{1}{(P(\omega_g))^2 \cdot Var^*(\omega_g)} \quad (3)$$

where

$$\mathrm{Var}^*(\omega_g) = \int_{-\infty}^{\infty} S(\omega; \omega_g)/S_0(\omega_g) d\omega \quad (4)$$

and $P(\omega_g)$ is the peak factor given by [16]

$$P(\omega_g) = \sqrt{2 \ln\left(2.8 \cdot \Omega(\omega_g) \cdot t_d/2\pi\right)} \quad (5)$$

where $t_d$ is the duration of the ground motion, and $\Omega(\omega_g)$ is given by

$$\Omega(\omega_g) = \sqrt{\frac{\int_{-\infty}^{\infty} \omega^2 S(\omega; \omega_g) d\omega}{\int_{-\infty}^{\infty} S(\omega; \omega_g) d\omega}} \quad (6)$$

It is also assumed that the standard deviation of the lognormal distribution of the power spectral density is constant with respect to $\omega$ and is equal to 0.4, and that the autocorrelation function of the power spectral density is modeled using the following equation [18]; the autocorrelation function of the response spectrum can be described by the function reported by Baker and Jayaram [19].

$$\rho_{\ln S^{1/2}(\omega_1), \ln S^{1/2}(\omega_2)} = 1 - 0.4 \cdot \left|\ln\left(\frac{\omega_1}{\omega_2}\right)\right| \quad (7)$$

The duration of the ground motions is assumed to be 40.96 s for intraplate earthquakes and 163.84 s for interplate earthquakes. The sampling frequency of the simulated ground motions is set to 50 Hz. The phase spectrum can be determined by the phase difference $\Delta\psi$. Iwata & Kuwayama [20] reported that the phase differences are normally distributed, and that their standard deviation $\sigma_{\Delta\psi}$ depends on the distance from the



 



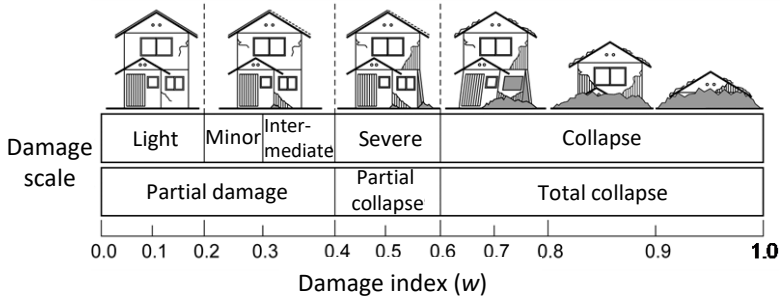


Fig. 3. Damage level and damage index [21]

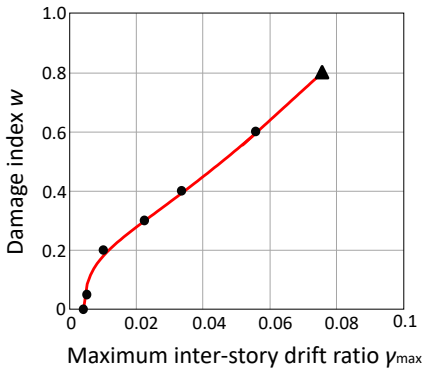


Fig. 4. Damage index as a function of $\gamma_{\max}$

Table 3. Damage level and maximum inter-story drift ratio

| Description of damage | Maximum inter-story drift ratio | | | | | | |
|---|---|---|---|---|---|---|---|
| | 1/250 | 1/200 | 1/120 | 1/45 | 1/30 | 1/18 | 3/40 |
| Condition of braces | | | Collapse deformation | Significant bending | Buckling of one brace | Buckling of more than one brace | |
| Damage index | 0.025 | 0.05 | 0.2 | 0.3 | 0.4 | 0.6 | 0.8 |

epicenter and is approximately equal to $0.025 \times 2\pi$ and $0.075 \times 2\pi$ for near-fault and near-to-medium-distance earthquakes, respectively. It is assumed here that $\sigma_{\Delta\psi}$ equals $0.025 \times 2\pi$ for half of the intraplate earthquakes and $0.075 \times 2\pi$ for the remainder, and that $\sigma_{\Delta\psi}$ equals $0.075 \times 2\pi$ for all the interplate earthquakes.

Six sets of 50 ground motions, simulated as described above, are then normalized such that the PGVs are equal to 0.5, 1.0, 1.5, 2.0, and 2.5 m/s. For structural models on medium and soft soils having $I_g$ equal to 0.3, 0.4, or 0.7 and subjected to interplate earthquakes, ground motions with PGV equal to 0.25 m/s are also considered.

### 2.5 Damage index and maximum inter-story drift ratio

Through nonlinear dynamic analysis (NDA), the response of a 2-DOF system, such as its maximum inter-story drift ratio ($\gamma_{\max}$), can be obtained, and then its damage level can be estimated. Here, damage is quantified using damage index, $w$, as shown in Fig. 3 [21]; the relationship assumed between $w$ and $\gamma_{\max}$ is shown in Table 3 [22]. It is assumed that the damage index is equal to 0.8 when $\gamma_{max}$ = 0.075, near which a structural model would lose its load-bearing capacity (Fig. 3). Then, the damage index is estimated as a function of $\gamma_{\max}$ using Eq. (8) (Fig. 4).

$$w = \frac{\sqrt{\ln(\gamma_{\max} \cdot 250)}}{6} + (\gamma_{\max})^{1.5} \cdot 25 \tag{8}$$

## 3. Results of Nonlinear Dynamic Analysis and Ground Motion Intensity

NDA rarely yields a damage index greater than or equal to 0.8, a value at which a structural model loses it load-bearing capacity; instead, it yields an error. Thus, the results of the analysis are classified into three groups: no damage ($w < 0.025$), damaged ($0.025 < w < 0.8$), and total collapse ($w > 0.8$).



 



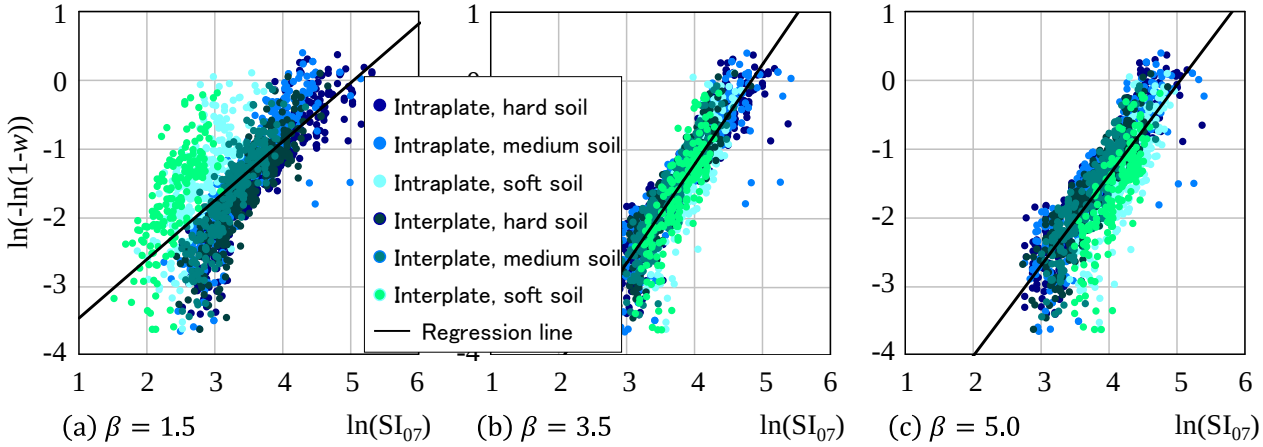


Fig. 5. Relationship between $\boldsymbol{X = \ln(SI_{I_g})}$ and $\boldsymbol{Y = \ln(-\ln(1-w))}$ $\boldsymbol{(I_g = 0.7)}$

### 3.1 Natural period-dependent spectrum intensity

Housner [23] proposed spectrum intensity (SI) as an integral of the velocity response spectrum with a damping of 20%, $Sv(T; h = 0.2)$, ranging from 0.1 s to 2.5 s. It can be used to estimate the damage level of a group of structures subjected to ground motions. However, it does not consider the characteristics of each structure. Kitahara and Itoh [10] proposed natural period-dependent SI, $SI_{\text{n.p.}}$ using integration in the range of $0.9T_1$ to $1.2T_1$ for a steel pier and $1.0T_1$ to $2.8T_1$ for an RC pier, where $T_1$ is the natural period of the structure. The upper and lower limits of the integration were determined based on NDA results using 15 piers and 72 ground motions, so that the correlation coefficient between $SI_{\text{n.p.}}$ and the maximum response of the piers was the highest (approximately 0.90–0.95). Based on this observation, natural period-dependent SI, $SI_{I_g}$, defined by the following equation, is used in this research to represent ground motion intensity.

$$SI_{I_g} = \frac{1}{\beta \cdot T_L - T_L} \int_{T_L}^{\beta \cdot T_L} Sv(T; h = 0.20)\, dT \tag{9}$$

where $T_L$ is the natural period of a wooden house roughly estimated as a function of its $I_g$, as shown in Table 1. The most appropriate upper limit of the integration, $\beta \cdot T_L$, is chosen among the values of $\beta$ (1.5, 2.0, 2.5, 3.0, 3.5, 4.0, and 5.0) such that the correlation between $SI_{I_g}$ and the damage level would be the highest.

### 3.2 Ground motion intensity for damage index function of “damaged houses”

It is assumed that the damage index function can be expressed in the form of Weibull distribution function similar to the one that uses PGV as the ground motion intensity [9]. Figures 5(a)–(c) show the relationship between $X = \ln(SI_{I_g})$ and $Y = \ln(-\ln(1-w))$ of the houses with $I_g = 0.7$, setting $\beta$ equal to 1.5, 3.5, and 5.0. The regression lines are also presented in the figures. It may be noted that regardless of the difference in the types of earthquakes, the results approximately align along the same straight line as long as the soil conditions are the same. On the contrary, the results of the group “soft soil conditions” shift from the left to the right as $\beta$ increases, while the results of the other groups remain relatively unchanged. For the soft soil conditions, the response spectrum generally retains relatively large value in the domain of long period. This observation suggests that there exists a value of $\beta$ leading to “universal” damage index functions that could be applied regardless of the soil conditions and the type of earthquake.

Figure 6 shows the correlation coefficient between $X = \ln(SI_{I_g})$ and $Y = \ln(-\ln(1-w))$ as a function of $I_g$ for various values of $\beta$. The correlation coefficients between $X = \ln(SI)$ and $Y$ and those



 



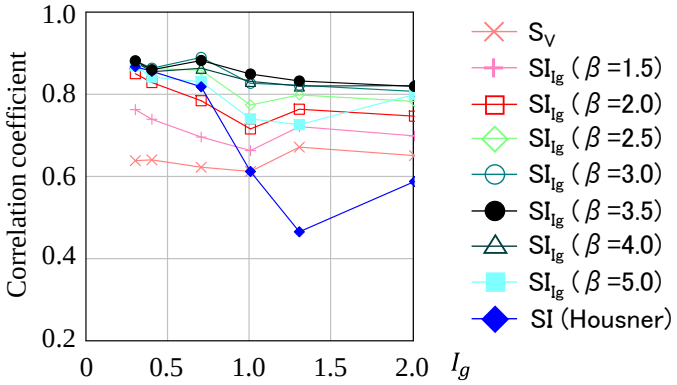


Fig. 6. Correlation coefficient between $\boldsymbol{X = \ln(SI_{I_g})}$ and $\boldsymbol{Y = \ln(-\ln(1-w))}$

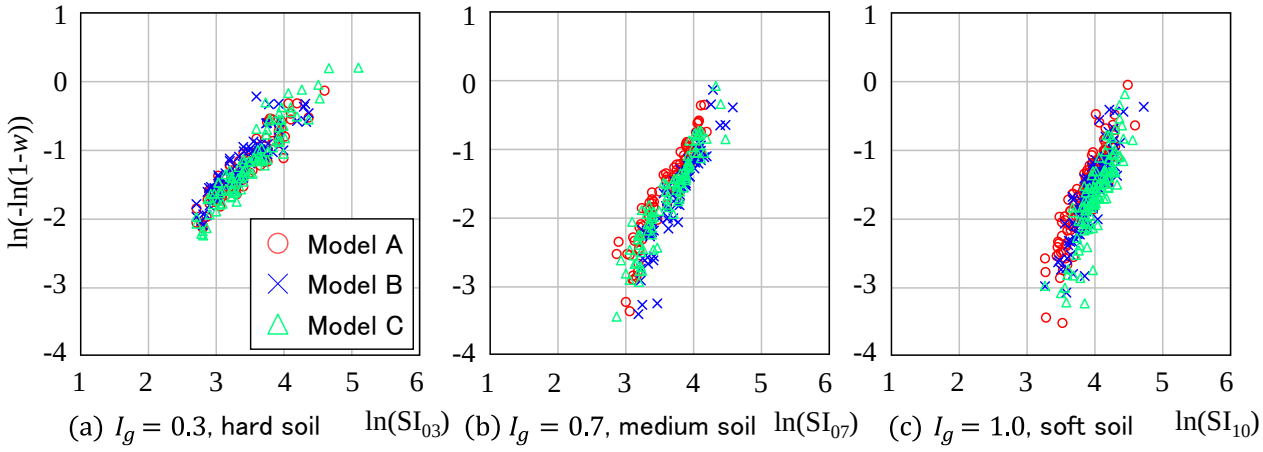


Fig. 7. Relationship between $\boldsymbol{X}$ and $\boldsymbol{Y}$ for each house model (intraplate)

between $\ln(Sv(T_1; h = 0.2))$ and $Y$ are also presented in the figure. It can be seen in the figure that the correlation coefficients depend on the value of $\beta$ and would be the highest in most cases when $\beta = 3.5$.

Figures 7(a)–(c) show the relationship between $X$ and $Y$ of each house model for $I_g$ equal to 0.3, 0.7, and 1.0, by setting $\beta = 3.5$. The results are aligned along the same line regardless of the type of the models. Based on these observations, it is proposed to use $SI_{I_g}$ with the range of integration from $T_1$ to $3.5 \cdot T_1$ as the intensity measure to estimate the damage level of wooden houses in Japan.

### 3.3 Damage index functions for wooden houses with $I_g$ used in NDA

As shown in Fig. 5, the damage index function can be expressed by a Weibull distribution function as

$$w = 1 - \exp\left[-\left(SI_{I_g}/u\right)^k\right] \tag{10}$$

where $k$ and $u$ can be estimated based on the parameters of the regressed straight line as shown in the figure. Figures 8(a)–(c) show the damage index functions (solid lines) for wooden houses with $I_g$ equal to 0.3, 0.7, and 1.0, along with the results of NDA.

In Fig. 5(b), the dispersion of the results along the regressed line is nearly uniform regardless of the values of $X = \ln(SI_{I_g})$, but slightly skewed. As similar tendency is observed in most cases, it is assumed here that the function $Y = \ln(-\ln(1-w))$ under the condition that $X = \ln(SI_{I_g})$ can be described by a shifted



 



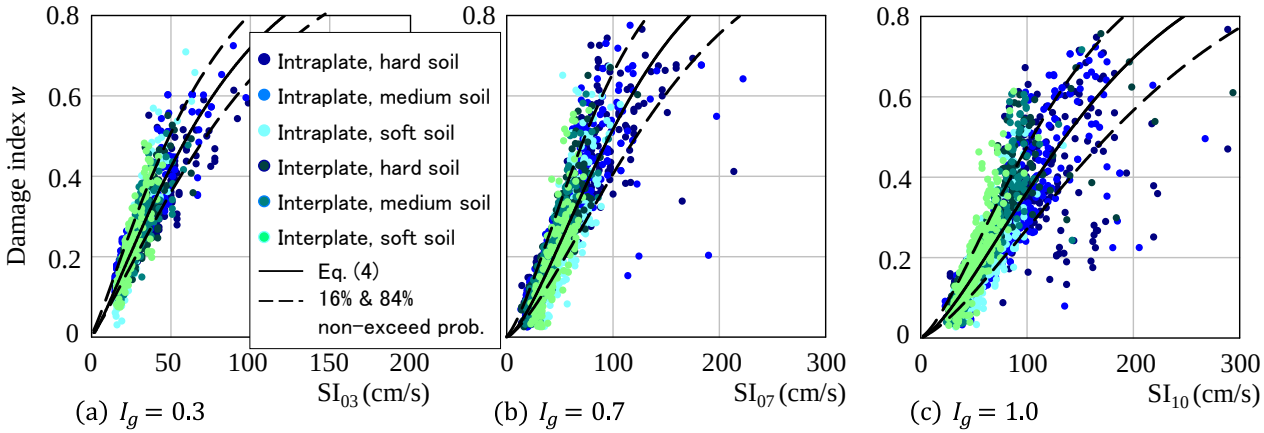


Fig. 8. Damage index, $\boldsymbol{w}$, as a function of $\boldsymbol{SI_{I_g}}$

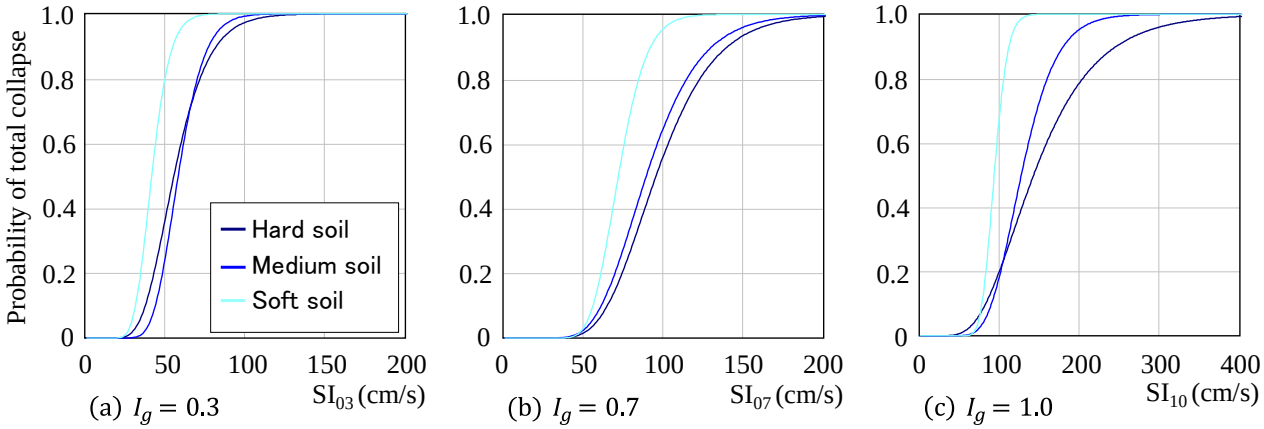


Fig. 9. Probability of total collapse as a function of $\boldsymbol{SI_{I_g}}$ (intraplate)

lognormal distribution function with uniform standard deviation, $\sigma_Y$, with a uniform shift equal to 4.0, and median equal to the vale estimated by Eq. (10). Using this dispersion model, the damage indices as a function $SI_{I_g}$ for non-exceedance values of 16% and 84% can be calculated using Eq. (10); the results are shown by dashed lines in Fig. 8.

### 3.4 Probability of total collapse

It is assumed that the probability of total collapse can be modeled by a lognormal distribution as a function of $SI_{I_g}$. The parameters of the distribution function are estimated by applying the maximum likelihood estimation [24] using the pairs of $SI_{I_g}$ and binary variables, $Z_C$, defined as

$$Z_C = \begin{cases} 0 & (w \le 0.8) \\ 1 & (w > 0.8) \end{cases} \tag{11}$$

By conducting similar investigations, it was found that the probability of total collapse can also be well explained by $SI_{I_g}$ with $\beta = 3.5$. Figures 9(a)–(c) show the probability of total collapse of the wooden houses with $I_g$ equal to 0.3, 0.7, and 1.0. Unlike the damage functions, the probability function of total collapse depends not only on $SI_{I_g}$, but also on soil conditions.

Whether a house would be damaged or not can be judged based on the elastic response spectrum. Once it is judged that a house is in the damaged or total collapse condition, the probability of total collapse is



 



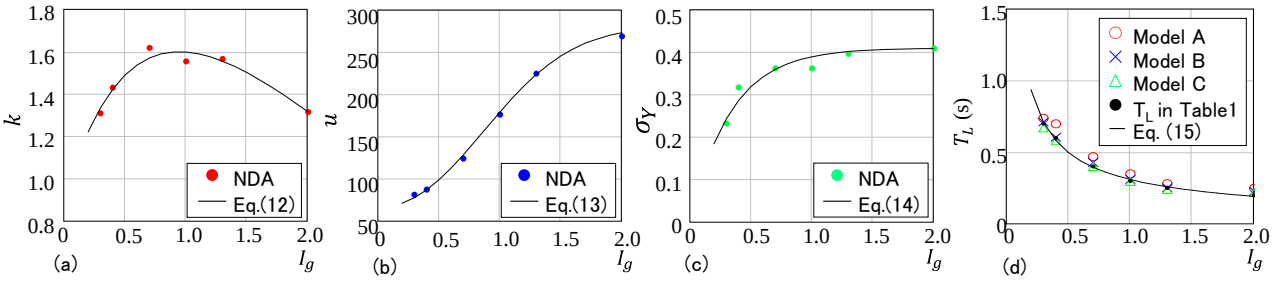


Fig. 10. Models of parameters for damage index function

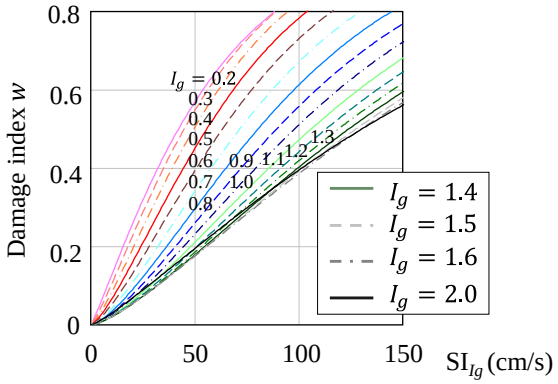


Fig. 11. Damage index with a non-exceedance probability of 90%

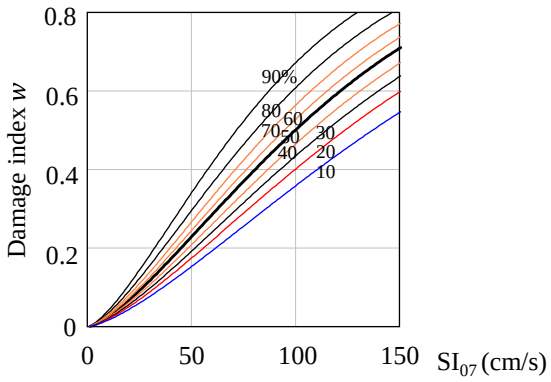


Fig. 12. Damage index with various non-exceedance probabilities, assuming $I_g = 0.7$

estimated as described in Sec. 3.4, and the level of damage is estimated under the condition of no total collapse as described in Sec. 3.3. From Figs. 8 and 9, it may be noted that even if the median of the damage index is relatively low, there is still a non-negligible probability of total collapse.

## 4. Modeling of Damage Index Functions

### 4.1 Damage index functions

The parameters of Eq. (10), $k$, $u$, standard deviation of $Y$ ($\sigma_Y$), and the lower limit of integration ($T_L$), for each group of wooden houses for different values of $I_g$ are presented in Fig. 10. To estimate the damage level of wooden houses with seismic grades other than those used in NDA, it is proposed to model these parameters as a simple function of $I_g$. These values are also shown in Fig. 10 by solid lines.

$$k = \frac{-0.531{I_g}^2 + 3.507I_g + 0.936}{\exp({I_g}^{0.65})} \tag{12}$$

$$u = 213\left(1 - \exp\left(-0.75{I_g}^{2.2}\right)\right) + 67 \tag{13}$$

$$\sigma_Y = 0.41(1 - \exp(-3.0I_g)) \tag{14}$$

$$T_L = 0.31{I_g}^{-0.687} \tag{15}$$

Figure 11 shows the damage index function with non-exceedance probability of 90% estimated using Eq. (10) and Eqs. (12)–(15) assuming that $I_g$ is in the range of 0.2–2.0. Figure 12 shows the damage index



 



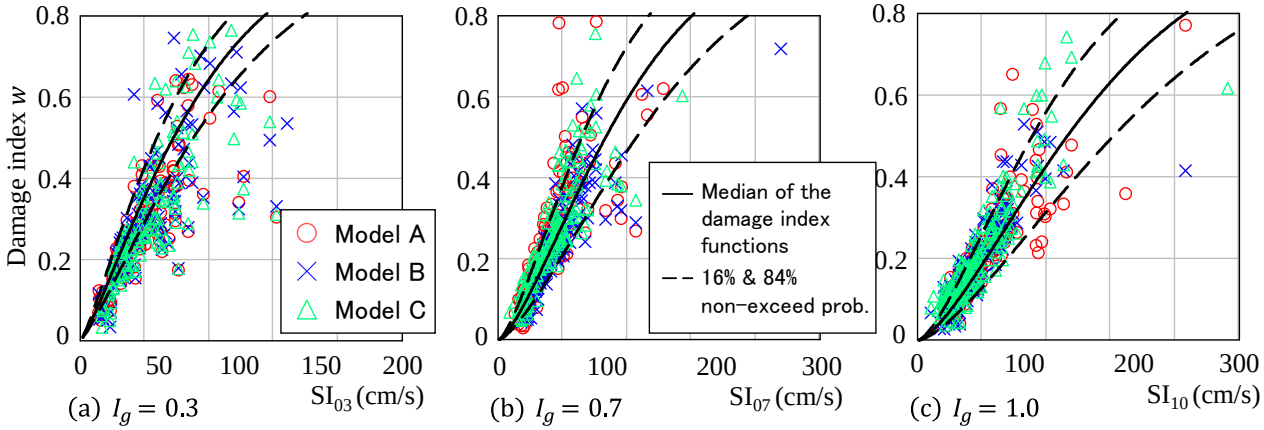


Fig. 13. Proposed damage index functions and NDA results using recorded ground motions

Table 4. Proportion of samples with non-exceedance values lying between 84% and 16%

| $I_g$ | 0.3 | 0.4 | 0.7 | 1.0 | 1.3 | 2.0 |
|---|---|---|---|---|---|---|
| Proportion of samples | 0.44 | 0.57 | 0.74 | 0.74 | 0.74 | 0.72 |

function with various values of non-exceedance probability with a 10% interval, assuming that $I_g = 0.7$. It should be noted that the range of integration for calculating $SI_{I_g}$, i.e. the horizontal axis in Figs. 11 and 12, depends on $I_g$ as defined by Eq. (9). Accordingly, $SI_{I_g}$ for a certain $I_g$ cannot be directly compared with that for another $I_g$.

## 4.2 Verification of proposed damage index functions

Using 128 ground motions recorded mainly in Japan and the United States of America, and those motions with intensities increased by a factor of two to obtain very large responses, the damage level of the three models described in Section 2.2 are estimated by NDA. Figures 13(a)–(c) show the results of NDA and the $SI_{I_g}$ of each ground motion for $I_g$= 0.3, 0.7 and 1.0. The figures show the median of the proposed damage index functions (solid line) and also damage index for the non-exceedance values of 16% and 84% (dashed lines). Table 4 summarizes the proportion of the samples with non-exceedance values lying in the range of 16–84%. Although this value is relatively low when $I_g$= 0.3, the samples fall reasonably within the range in the other cases.

## 4.3 Comparison with damage index model as a function of PGV

The dispersions of the damage index estimated by the proposed damage index function, which uses natural period-dependent spectrum intensity as ground motion intensity, are investigated by comparing them with the values reported in the paper by Mori et al., in which PGV is used as the ground motion intensity (referred to hereafter as Mizutani model) [9]. Because the scale of ground motion intensity in these two models cannot be compared directly, the dispersions are measured by the non-exceedance values lying in the range of 16–84% for a certain median of the damage index. Figures 14(a)–(c) show the range of the non-exceedance values in the proposed model with the median of damage index equal to 0.2, 0.4, and 0.6, along with those in Mizutani model. The dispersions of the proposed damage index function are at the most half of those in Mizutani model, and could be much smaller when $I_g$ is low, showing a significant improvement from Mizutani model.



 



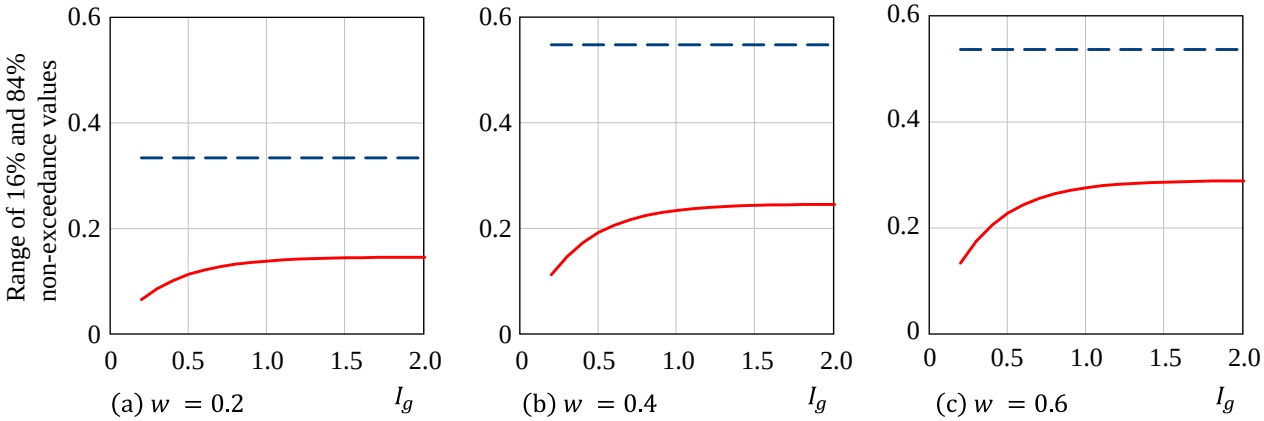


Fig. 14. Dispersion of damage index function for non-exceedance values lying in the range of 16–84%

## 5. Summary

In this paper, a probabilistic damage index function for the two-story wooden houses commonly constructed in Japan is proposed based on the results of NDA, using a number of ground motions simulated considering various soil conditions and types of earthquakes. Three existing two-story wooden houses with typical seismic resistance elements, used in construction in the 1960s and the 1970s, are considered. These houses are upgraded or downgraded by adding or removing walls and/or braces to the model houses with various levels of load-carrying capacity. It is proposed to use the natural period-dependent spectrum intensity, $SI_{I_g}$, with the range of integration from the estimated natural period, $T_L$, to $3.5 \cdot T_L$ as the ground motions intensity to take the structural characteristics of houses into account. The previously developed damage index functions that use PGV as the ground motion intensity require judgement of the soil condition and the type of earthquake. On the contrary, the proposed damage index functions are universal, and are independent of the soil condition and the type of earthquake. Further, the dispersion of the proposed damage index function is much smaller than that of the previously developed one. However, the probability of total collapse depends not only on $SI_{I_g}$ but also on soil conditions, and further research is required for appropriate modeling.

## 6. References

[1] ASCE. (2009) *Policy Statement 390 - Earthquake Hazards Mitigation*, http://www2.asce. org/Content.aspx?id= 8361.

[2] ATC-71. (2009) *NEHRP Workshop on Meeting the Challenges of Existing Buildings, Part 2: Status Report on Seismic Evaluation and Rehabilitation of Existing Buildings*, pp.110.

[3] Wen, Y.K., Ellingwood, B.R. (2005) "The Role of Fragility Assessment in Consequence-Based Engineering," *Earthquake Spectra*, 21(3), pp.861-877.

[4] Shakib, H., Joghan, S.D., Pirizadeh, M. (2011) "Proposed Seismic Risk Reduction Program for the Megacity of Tehran, Iran," *Natural Hazards Review*, ASCE, 12(3), pp.140-145.

[5] Mori, Y., Yamaguchi, T., Idota, H. (2012) "Risk-based Strategies for Upgrading Existing Non-conforming Wooden Houses and Risk Information for Promoting Upgrading," *Natural Hazards Review*, ASCE, 13(3), pp.179-187.

[6] Miyakoshi, J., Hayashi, Y., Tamura, K., N. Fukuwa, N. (1997) "Damage Ratio Functions of Building using Damages Data of the 1995 Hyogo-ken Nanbu Earthquake," *Proc. 7th Int. Conf. Structural Safety and Reliability*, pp.349-354.

[7] Murao, O., Yamazaki, F. (2002) "Building Fragility Curves for the 1995 Hyogoken-Nanbu Earthquake Based on CPIJ & AIJ'S Survey Results with Detailed Inventory", *J. Struct. Constr. Eng.*, 555, pp.185-192. (in Japanese)



 



[8] Mizutani, Y., Sugai, M., Mori. Y. (2017) "Application of Modified Kriging Method to Estimations of Earthquake Ground Motion Intensity at Construction Sites," *Safety, Reliability, Risk, Resilience and Sustainability of Structures and Infrastructure*, pp.3259-3269.

[9] Mori, Y., Mizutani, Y., Kang, J. D., Idota, H. (2018) "Upgrade Decision-making for Earthquake-vulnerable Wooden Houses using Probabilistic Damage Index Functions," *ASCE-ASME Journal of Risk and Uncertainty in Engineering Systems, Part A: Civil Engineering*, ASCE.

[10] Kitahara, T., Itoh, Y. (1999) "A Correlation between Elasto-plastic Dynamic Response of Steel and RC Piers and Natural Period-dependent Spectrum Intensity," *Journal of Structural Engineering*, Vol.45A, pp.829-838, 1999 (in Japanese).

[11] Idota, H., Mineoka, S., Umemura, H., Mori, Y. (2007) "Relationship Between Seismic Capacity Grade and Damage for Post and Beam Wooden Structures, A Study on Decision-making Tools for Promoting Aseismic Reinforcement of Old Wooden Houses (Part 1)," J. Struct. Constr. Eng., 612, pp.125-132. (in Japanese)

[12] Matsunaga, H., Miyadu, Y., Soda, S. (2008). "Time history seismic response analysis for wooden structure applied extended NCL model." *Summaries of Technical Papers of Annual Meeting Architectural Institute of Japan*, AIJ, Tokyo, 181–182. (in Japanese)

[13] Isoda, H., Hirano, S., Miyake, T., Furuya, O., Minowa, C. (2007) "Collapse Mechanism of New Wood House Designed According with Minimum Seismic Provisions of Current Japan Building Standard Law," J. Struct. Constr. Eng., 618, pp.167-173. (in Japanese)

[14] Takada, K., Isoda, H., Tsuchimoto, T., Kawai, N., Nakagawa, T., Sugimoto, K., Aoki, K., Ozawa, A., Wakabayashi, D. (2010) "Static Loading Test of Existing Wood House in Cottage Area," Proc. *Annual Meeting of Hokuriku Chapter*, AIJ, 53, pp.159-162. (in Japanese)

[15] Iyama, J. (2012) "Study on Probability Distribution of Residual Deformation of Elastic-perfectly Plastic SDOF System after Earthquakes based on Assumption of Random Walk," *J. Struct. Constr. Eng.*, 674, pp.537-544. (in Japanese)

[16] Hamaguchi, H., Kanda, J. (1994) "Proposal of the Simulated Ground Motion with Long-period Components Reduced Kanai-Tajimi Power Spectrum," *Summaries of Technical Papers of Annual Meeting, AIJ (Tokai)*, pp.399-400. (in Japanese)

[17] Monti, G., Nuti, C., Pinto, P.E. (1996) "Nonlinear Response of Bridges under Multi-support Excitation", *J. Structural Engineering*, 122, pp.1147-115.

[18] Okano, S., Ishida, H., Kato, K. (2010) "Theoretical Study on Inter Period Correlation of Residuals of Ground Motion Prediction Equation," *J. Struct. Constr. Eng.*, 655, pp.1617-1624.

[19] Baker, J.W., Jayaram, N. (2008) "Correlation of Spectral Acceleration Values from NGA Ground Motion Models." *Earthquake Spectra*, 24(1), pp.299-317.

[20] Iwata, Y., Kuwamura, H. (2003) "Earthquake Input Motions in Performance Evaluation of Steel Building Structures, Part 3: Simulated Earthquake Motions for Performance Evaluation," *Proc. Annual Meeting of Hokuriku Chapter*, AIJ, 73, pp.137-140.

[21] Okada, S., Takai, N. (2004) "Damage Index Functions of Wooden Buildings and Reinforced Buildings for Seismic Risk Management," Proc. 13th World Conference on Earthquake Engineering, Paper No.727, pp.10.

[22] General Insurance Rating Organization of Japan (2010) Study on Estimation of Damage of Buildings Considering Aftershocks, pp.91. (in Japanese)

[23] Housner, G.W. (1961) "Vibration of Structures Induced by Seismic Waves," *Vibration Handbook*, Harris, C.M. and Crede, C.E. (eds.) Vol.3, pp.1-32.

[24] Mochizuki, T., Nakamura, T. (2000) "Statistical Estimation of Seismic Fragility Curves by Polynomial Likelihood Model," Proc. the Second Real-time Earthquake Disaster Prevention Symposium, pp.47-50.



 